Effect of Ag on the Oxidation of β-NiAl at 1173 to 1373K in 10^5Pa Oxygen Atmosphere

X. J. Zhang[°*#], Z. G. Zhang[°] and Y. Niu[*]

[°]*Shenyang Institute of Chemical Technology, 110142 Shenyang, China*
[*]*State Key Laboratory for Corrosion and Protection, Institute of Metal Research, Chinese Academy of Sciences, Wencui Road 62, 110016 Shenyang, China*

(Received August 29, 2005; final form September 7,2005.)

ABSTRACT

Oxidation of two ternary NiAl-Ag alloys containing 0.5, 1 at.% Ag, denoted as NiAl-0.5Ag and NiAl-1Ag, and Ag-free β-NiAl was studied at 1173, 1273, and 1373K for 24 h in 10^5Pa O_2 to study the effect of the presence of silver on the oxidation behavior of β-NiAl by TGA, XRD, and SEM/EDAX. The NiAl-Ag alloys contain a mixture of a silver-rich phase (α) and a matrix of nickel-aluminide NiAl (β). Thus, these alloys are ternary two-phase systems containing two reactive elements plus a noble metal. Under the oxygen pressure used, nickel and aluminum can form stable oxides, while silver is noble. An exclusive and adhesive external Al_2O_3 scale formed on the β-NiAl, NiAl-0.5Ag, and NiAl-1Ag alloys after 24h oxidation in 10^5Pa O_2 at 1173 and 1273K. Some voids were observed at the interface of oxide and alloy containing silver and silver free NiAl at 1373K. The oxidation kinetics of the two alloys at 1173K and 1373K is similar to that of β-NiAl. The initial oxidation rate of NiAl-0.5Ag and NiAl-1Ag at 1373K is similar to that of β-NiAl. After 4h oxidation at 1373K the alloys containing silver begin to show mass loss. The addition of silver does not affect significantly the oxidation behavior of the NiAl intermetallic compound in all cases, as expected, because silver is essentially present only as a second phase due to its very small solubility in β-NiAl.

Key words: β-NiAl, Ag addition, High temperature oxidation

1. INTRODUCTION

NiAl intermetallic compound is being considered as a material for high temperature applications, due to the combination of its low density, high melting point, and high thermal conductivity, and in particular to its excellent oxidation resistance, which is attributed to aluminum oxide formation over a wide range of temperatures and oxygen pressures /1-4/. However, the poorness of its room-temperature ductility and high temperature strength is a significant obstacle to the alloy's structural use. Nevertheless, significant progress has been achieved in improving the ambient and elevated temperature properties of the compound by several methods. The result of adding Ag to NiAl is that a minor amount (<1 at.%) of Ag addition increased its strength and improved NiAl's room temperature compressive ductility /5/. High hardness, high electrical conductivity and some room temperature ductility combined with the advantages mentioned above make NiAl-Ag a candidate for electrical contact material /5/. It is noted that the effect of Ag addition on the oxidation behavior of β-NiAl intermetallics is still unknown. The oxidation of the three present alloys has been carried out

Correspondent: zhangxuejun@syict.edu.cn (Dr. X. J. Zhang) or zhxj890@sohu.com

in 10^5Pa O_2 at 1173-1373K with the aim to illustrate the effect of minor Ag addition on the oxidation behavior of β-NiAl intermetallic compound.

2. EXPERIMENTAL

β-NiAl, NiAl-0.5Ag and NiAl-1Ag alloy ingots were arc melted under an argon atmosphere on a water-cooled copper crucible using the original materials of nickel (99.99%), aluminum (99.999%), and Ag (99.99%). Each button was inverted and remelted three times in order to ensure the homogeneity. The alloys were subsequently annealed for 30h at 1473K in argon atmosphere followed by furnace cooling to remove residual mechanical stresses and to achieve a better equilibration of the alloy phases. The actual composition in at% of the samples investigated is listed in Table 1. Figure 1 shows the microstructure of NiAl-0.5Ag and NiAl-1Ag. At room temperature, NiAl-0.5Ag and NiAl-1Ag alloys contain two phases, one of which is the NiAl (β phase) with small silver content (about 0.3at% according to the EDS results), while the other phase is mostly composed of silver solid solution (α phase) with a small content of nickel and aluminum.

Table 1
Composition in at% of the samples investigated

Alloys	Element		
	Ni	Al	Ag
β-NiAl	51.58	49.42	-
NiAl-0.5Ag	50.01	49.71	0.51
NiAl-1Ag	49.94	49.77	0.83

Flat specimens with a surface area of about $2x10^{-4}$ cm^2 were cut from the ingots by an electric spark cutting, abraded on SiC paper successively down to 1200 grade, degreased in water and acetone, ultrasonically cleaned with alcohol, and dried immediately before use. Oxidation tests were carried out in 10^5Pa O_2 at 1173, 1273, and 1373K for 24h to examine the effect of minor silver addition to NiAl on isothermal oxidation of β-NiAl. The microstructure of the alloys and the oxide scales was characterized by X-ray diffraction (XRD) and by Scanning Electron Microscopy (SEM) with attached energy-dispersive spectroscopy (EDS) to establish the nature, composition, and spatial distribution of the compounds formed by oxidation.

3. RESULTS

3.1 Scaling kinetics

Plots of the mass gain versus time and mass gain versus square root of time for the three alloys containing silver and silver free at 1173, 1273 and 1373K are shown in Figure 2 to Figure 4 respectively, and the k_p values of the three alloys at different temperatures are listed in Table 2. At 1173K, the oxidation rate of the two alloys containing silver is a little greater than that of β-NiAl, but the parabolic plots indicate that the kinetics of the three alloys can be described as two main stages with a slightly smaller rate constant for the second stage than the first one (Figure 2b). At 1273K, the oxidation kinetics of NiAl-0.5Ag, NiAl-1Ag and β-NiAl can also

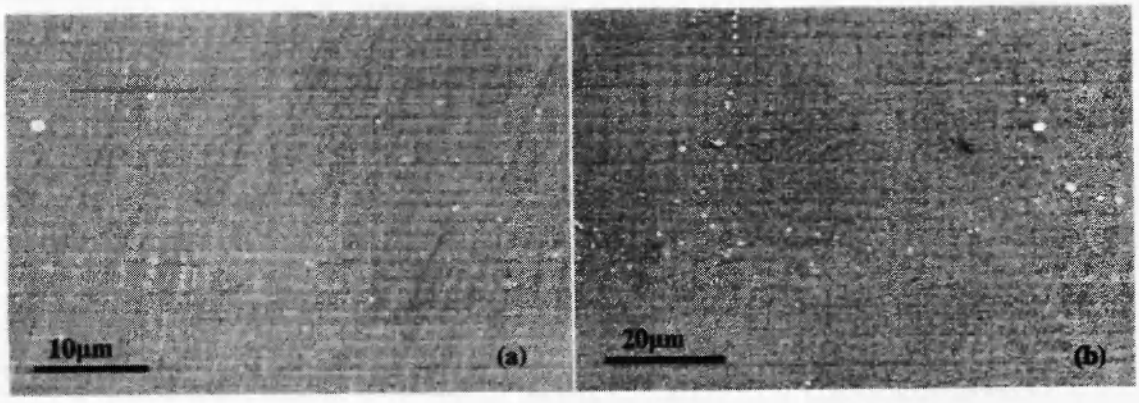

Fig. 1: Microstructure (SEM/BEI) of (a) NiAl-0.5Ag and (b) NiAl-1Ag

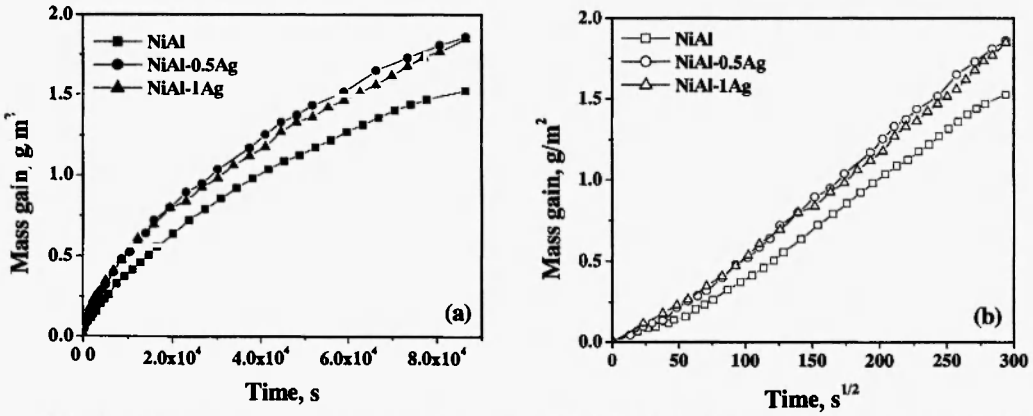

Fig. 2: Kinetics curves for the oxidation of NiAl, NiAl-0.5Ag, and NiAl-1Ag at 1173K in 10^5Pa O_2, (a) Normal plots; (b) Parabolic plots.

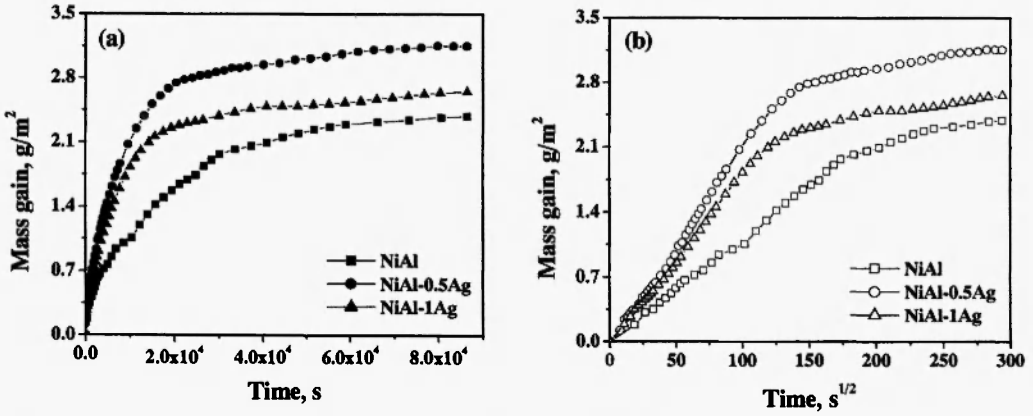

Fig. 3: Kinetics curves for the oxidation of NiAl, NiAl-0.5Ag, and NiAl-1Ag at 1273K in 10^5Pa O_2, (a) Normal plots; (b) Parabolic plots.

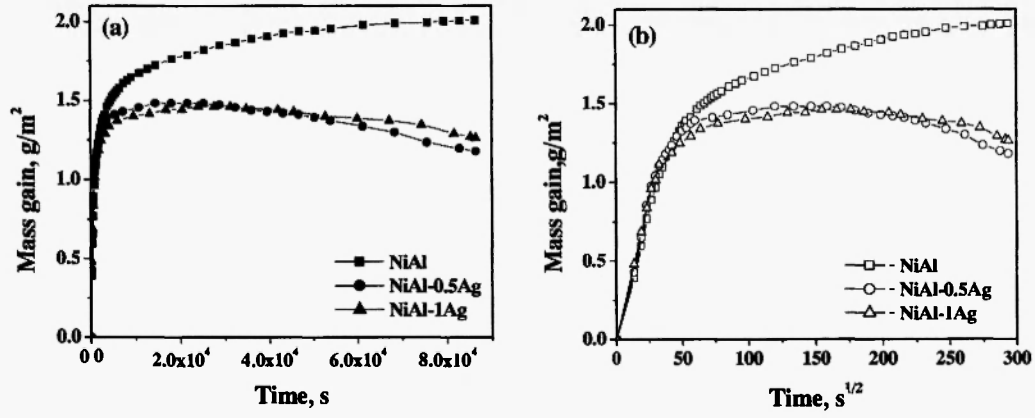

Fig. 4: Kinetics curves for the oxidation of NiAl, NiAl-0.5Ag, and NiAl-1Ag at 1173K in 10^5Pa O_2 , (a) Normal plots; (b) Parabolic plots.

Table 2
Parabolic rate constants (all k_p values in g^2cm^{-4} s^{-1}) for the oxidation of the three alloys in different stages in 10^5Pa O_2 at 1173 and 1373K

Alloys	1173 K		1273 K		1373 K	
	k_p (in)	k_p (fi)	k_p (in)	k_p (fi)[]	k_p (in)[]	k_p (fi)[]
NiAl	1.12×10^{-5}	3.72×10^{-5}	3.24×10^{-4}	3.10×10^{-6}	9.38×10^{-4}	8.16×10^{-6}
NiAl-0.5Ag	2.33×10^{-5}	4.97×10^{-5}	4.44×10^{-4}	8.996×10^{-6}	1.01×10^{-3}	-
NiAl-1Ag	2.69×10^{-5}	4.64×10^{-5}	3.24×10^{-4}	6.92×10^{-6}	1.16×10^{3}	-

(in): values in initial stage; (fi): values in final stage

be described as two different parabolic stages and the second parabolic rate constant is smaller by about two orders of magnitude than the first ones. The initial oxidation rate constant of NiAl-0.5Ag and NiAl-1Ag is very similar to that of β-NiAl and the final rate constants of NiAl-0.5Ag and NiAl-1Ag are a little greater than that of β-NiAl. At 1373K, the oxidation kinetics of β-NiAl can be described as two different parabolic stages and the second parabolic rate constant is smaller than the first one. The initial oxidation rate of NiAl-0.5Ag and NiAl-1Ag is similar to that of β-NiAl, after 4h oxidation at 1373K the alloys containing silver begin to show weight loss gradually due to the volatilization of silver.

3.2 Surface morphology

X-Ray diffraction results of the oxide on the three alloys after 24h oxidation at different temperatures are listed in Table 3. After 24h oxidation at 1173K, the surface morphologies of the oxides formed on the three alloys are shown in Figure 5 respectively. The oxide formed on β-NiAl (Figure 5a) is whisker-like disorderly which should be related to metastable alumina such as θ-Al_2O_3 characterized by means of TEM and XRD /6,7/. The oxides formed on the two alloys containing silver are still whisker-like, but the whisker or blade is shorter and finer than that formed on β-NiAl (Figure 5b and c). The topographies of the oxides formed on the three alloys at 1273K are shown in Figure 6 respectively. After 24h exposure, for β-NiAl alloy, whisker- or blade-like metastable θ-Al_2O_3 distributed at the scale-gas interface and no α-Al_2O_3 was observed on the surface by means of SEM. Whereas the surface oxide of NiAl-0.5Ag and NiAl-1Ag is flat plate in most locations, which is corresponding to "intrinsic" α-Al_2O_3 /6,7/, and only a very little metastable θ-Al_2O_3 was found whose quantity was lower than the analysis sensitivity of XRD (Table 3). After 24h oxidation at 1373K, two types of oxides were observed on the surface of NiAl i.e. whisker-like metastable θ-Al_2O_3 and stable α-Al_2O_3, as shown in Figure 7a. The "extrinsic" type α-Al_2O_3 and a very few fine θ-Al_2O_3 particles (Figure7b and c) were formed on the NiAl-Ag alloy.

3.3 Cross-sectional morphology

The scales formed on β-NiAl and NiAl-Ag alloys after oxidation 24h in 10^5Pa O_2 at 1173K are shown in Figure 8 respectively. An exclusive and continuous

Table 3
X-Ray diffraction results of the oxide on the three alloys after 24h oxidation at different temperatures

	NiAl	NiAl-0.5Ag	NiAl-1Ag
1173K	θ-Al_2O_3, α-Al_2O_3	θ-Al_2O_3, α-Al_2O_3	θ-Al_2O_3, α-Al_2O_3
1273K	α-Al_2O_3 θ-Al_2O_3	α-Al_2O_3	α-Al_2O_3
1373K	α-Al_2O_3 θ-Al_2O_3	α-Al_2O_3	α-Al_2O_3

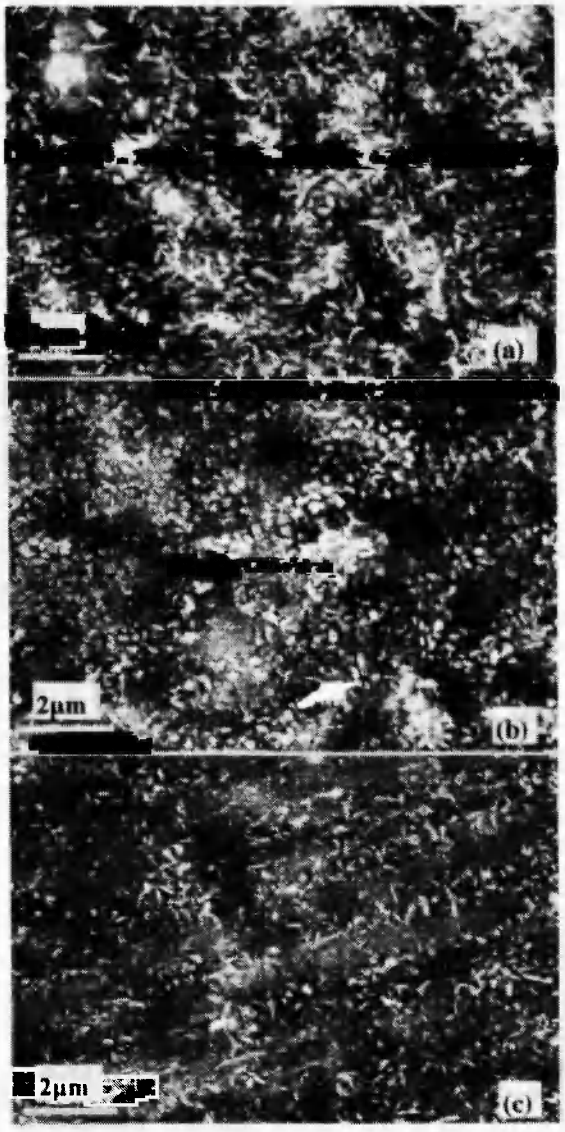

Fig. 5: Surface morphologies of scales formed on the three alloys after 24h oxidation at 1173K. (a) β-NiAl, (b) NiAl-0.5Ag, (c) NiAl-1Ag.

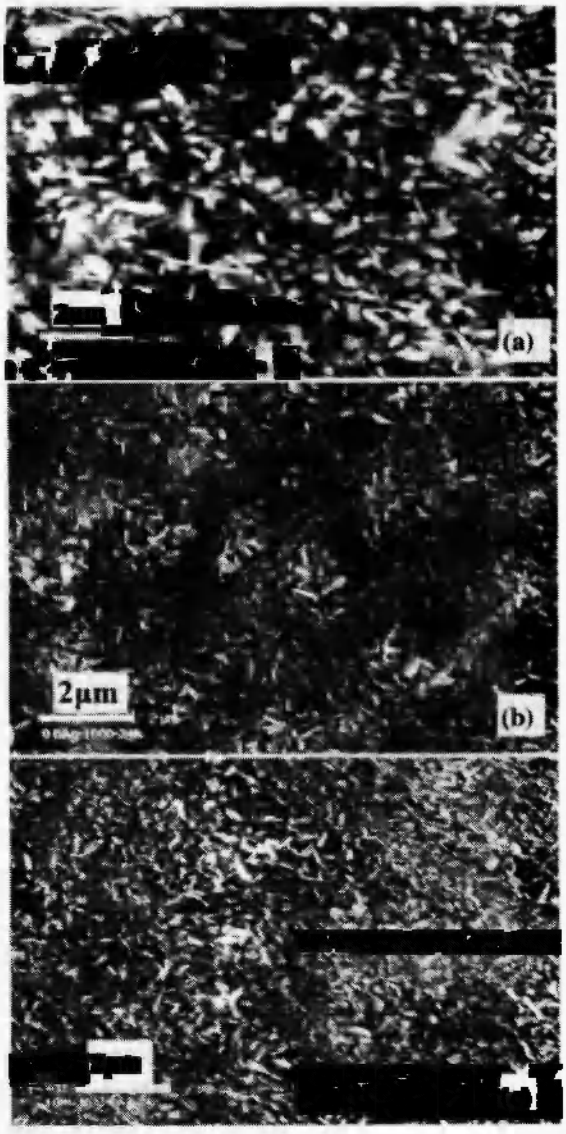

Fig. 6: Surface morphologies of scales formed on the three alloys after 24h oxidation at 1273K. (a) β-NiAl, (b) NiAl-0.5Ag, (c) NiAl-1Ag.

Al_2O_3 layer was formed and the alumina scale fits the alloy substrate closely and no voids are present. In the case of 24h oxidation at 1273K (Figure 9), some voids were observed at the scale/alloy interface for NiAl and NiAl-0.5Ag alloy, while the situation was the opposite apart from a very few silver particles embedded at the interface of alumina and NiAl-1Ag alloy substrate. After 24h oxidation at 1373K, many voids formed at the interface of scale and alloy substrate for the three alloys, as shown in Figure 10.

4. DISCUSSION

Of the three binary systems connected with the present ternary alloys, nickel and aluminum form a

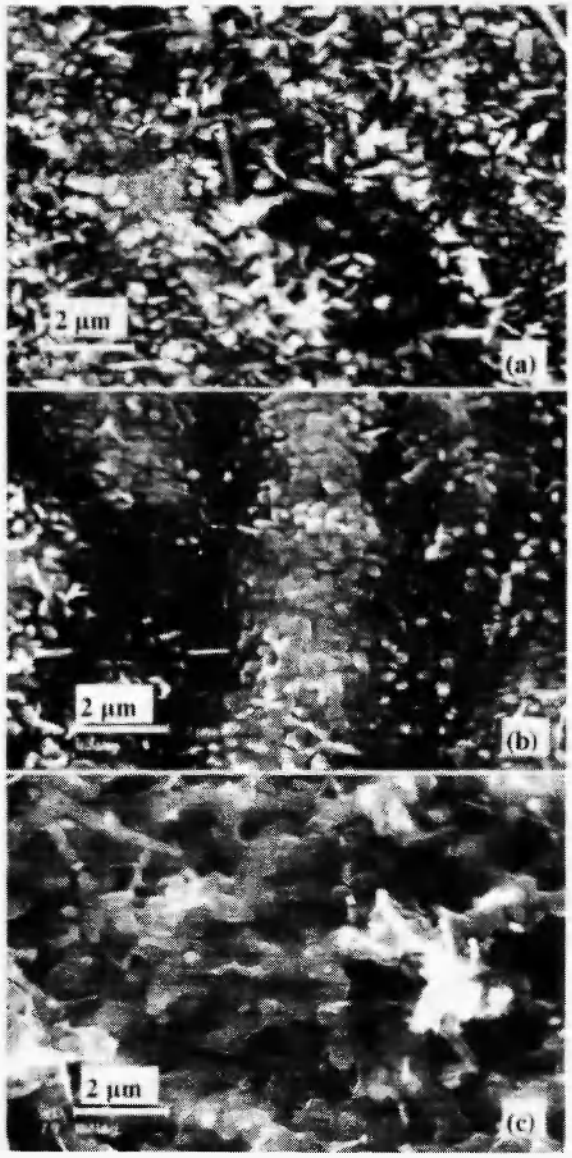

Fig. 7: Surface morphologies of scales formed on the three alloys after 24h oxidation at 1373K. (a) β-NiAl, (b) NiAl-0.5Ag, (c) NiAl-1Ag.

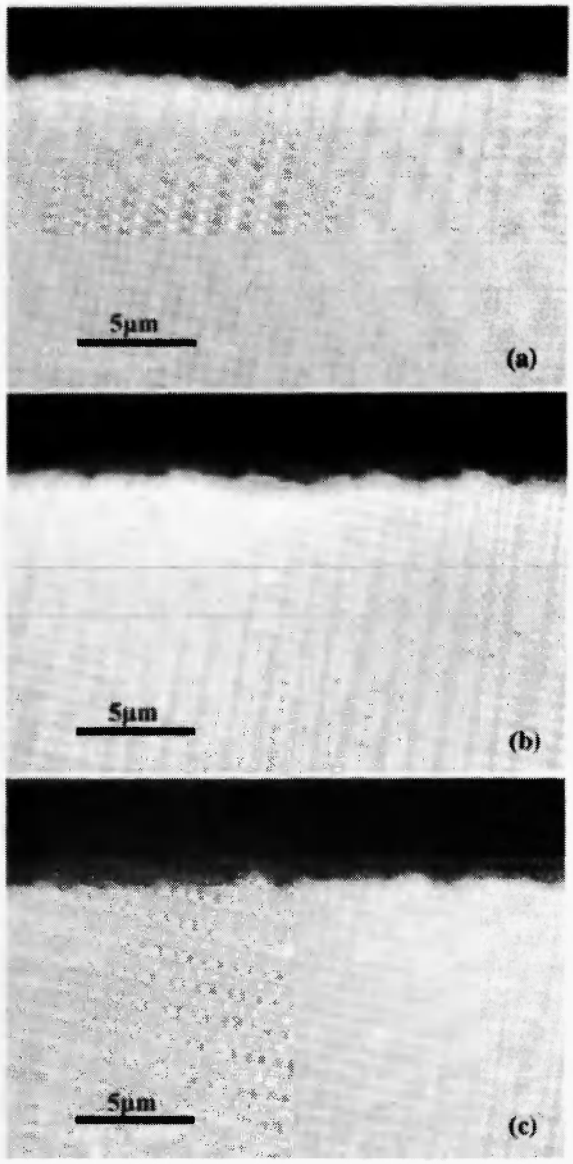

Fig. 8: Cross-section (SEM/BEI) of (a) NiAl, (b) NiAl-0.5Ag, and (c) NiAl-1Ag oxidized in 10^5 Pa O_2 at 1173K for 24h.

continuous series of solid solutions in a large composition range, while nickel and silver and aluminum and silver have a very limited mutual solubility, so that both Ni-Ag and Al-Ag are two-phase in almost all their composition range. The scaling behavior of NiAl is briefly recalled before considering that of the present alloys. The oxidation behavior of Ni-Al alloys has been investigated extensively. Pettit /8/ systematically studied the oxidation of Ni-3 to 25 mass% Al in 0.01 MPa oxygen between 1173 and 1573K. He found that the higher the temperature the greater was the tendency to form and maintain external α-Al_2O_3 scale, while the oxidation mechanism depended on the alloy composition and temperature. According to Wood and Stott /9/, who examined in detail the oxidation of Ni-7 mass% Al and Ni-12.5

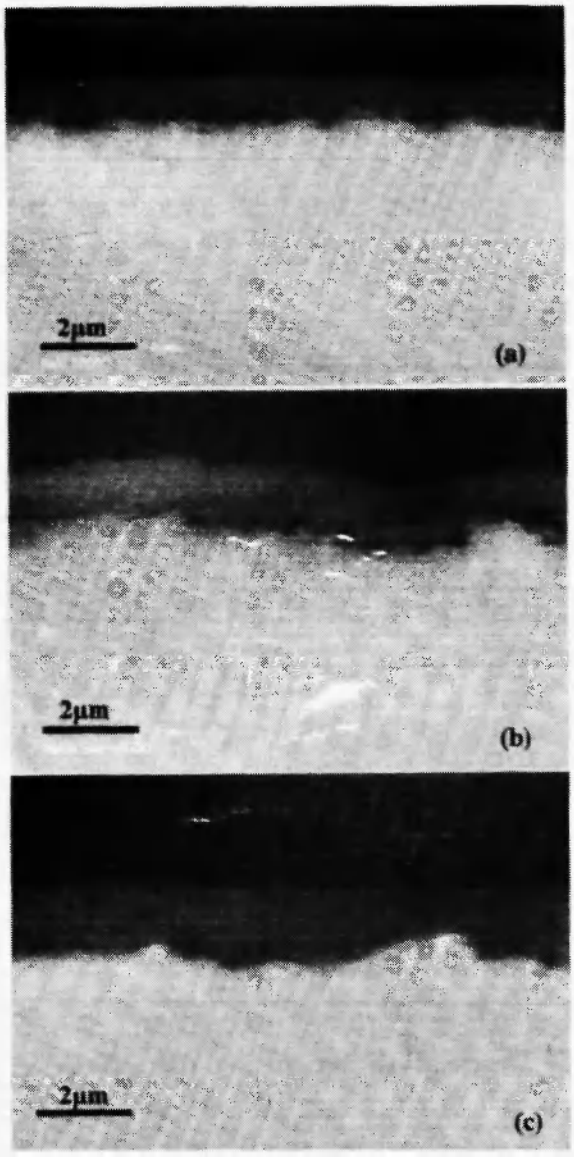

Fig. 9: Cross-section (SEM/BEI) of (a) NiAl, (b) NiAl-0.5Ag, and (c) NiAl-1Ag oxidized in 10^5 Pa O_2 at 1273K for 24h.

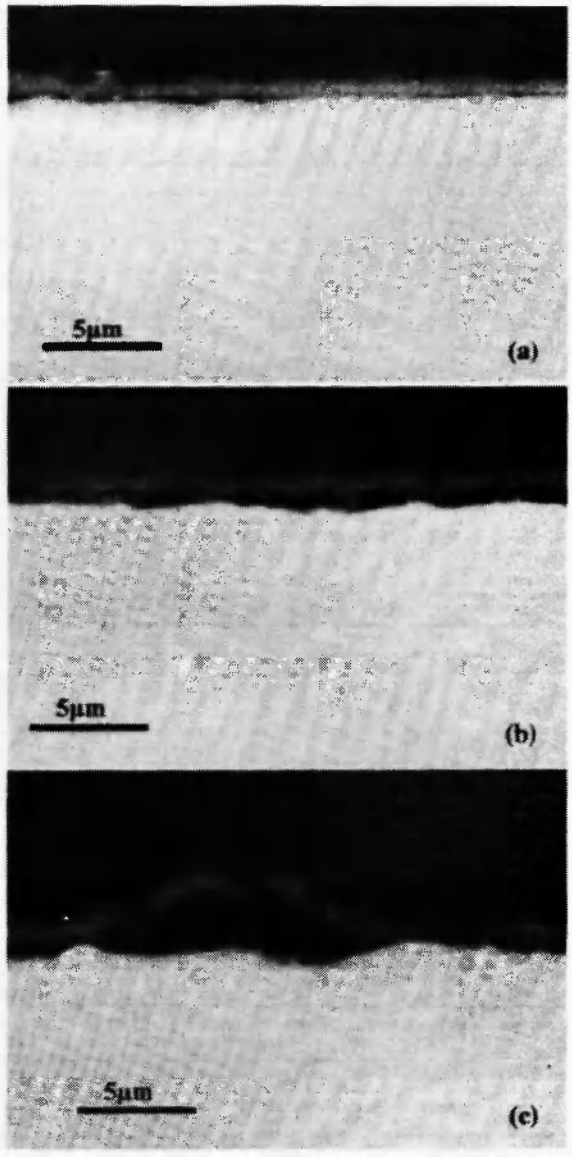

Fig. 10: Cross-section (SEM/BEI) of (a) NiAl, (b) NiAl-0.5Ag and (c) NiAl-1Ag oxidized in 10^5 Pa O_2 at 1373K for 24h.

mass% Al in 0.1MPa oxygen at 1073 to 1473K, the α-Al_2O_3 external scale forms more easily at higher aluminum contents and at higher temperatures because aluminum in the substrate can diffuse to the alloy/oxide interface more readily. The external α-Al_2O_3 scale tended to fail mechanically locally, after which Ni-12.5 mass% Al succeeded in re-forming α-Al_2O_3, while Ni-7 mass% Al produced non-protective NiO-rich nodules, subsequently healed by new α-Al_2O_3 layers. Grabke *et al.* /10-15/ systematically studied the kinetics of alumina growth on β-NiAl alloys in the temperature range 973-1673K. Their results indicated that a slight increase of k_p values was observed during the first 10-20h due to the formation of θ-Al_2O_3 from γ-Al_2O_3. However, when the transformation between θ-Al_2O_3 to α-Al_2O_3 took place, in the temperature range 1223-1323K, the k_p

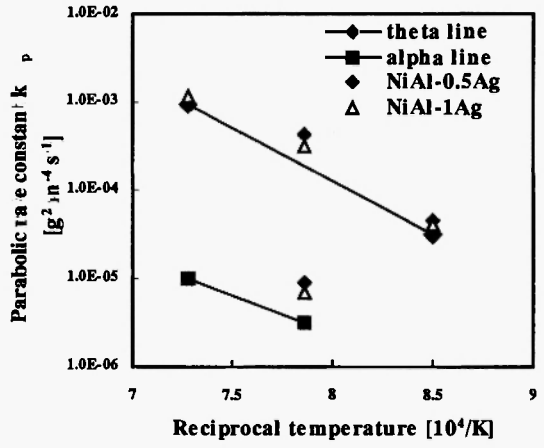

Fig. 11: Arrhenius diagram of k_p for oxidation in the temperature range 1173-1373K

values obviously decreased.

In agreement with the literature /10-13/, the oxidation rate depends on the oxidation temperature and oxidation time. At 1173K, the parabolic plots of the three present alloys exhibit two stages and the parabolic rate constant for the second stage is a little greater than that for the first one, which indicates that the oxidation followed the same mechanism i.e. the growth of metastable γ-Al_2O_3 and then transformation to θ-Al_2O_3 very quickly. At 1273K, the kinetics curve of β-NiAl alloys is composed of two stages and the second parabolic rate constant is smaller two orders of magnitude than that for the first stage. The scaling rates of the NiAl-0.5Ag and NiAl-1Ag alloys are substantially similar to those for the oxidation of NiAl in spite of the presence of small amount of silver. This change in rate at 1273K was attributed by Rybicki and Smialek /6/ to the change from metastable alumina formation to a slow growing α-Al_2O_3 scale. At 1373K, the kinetics curve of β-NiAl is composed of two parabolic stages, which is also attributed to the change from metastable alumina formation to a slow growing α-Al_2O_3 scale. The oxidation behavior of NiAl-0.5Ag and NiAl-1Ag at 1373K is different from that of β-NiAl. The oxidation behavior of NiAl-0.5Ag and NiAl-1Ag at the first 1h is similar to that of β-NiAl, and the weight gain becomes negative after the initial oxidation due to the volatilization of Ag under the present temperature. By comparison of Figure 4b with 3b, the oxidation kinetics of the three present alloys shows the phase transformation from θ-Al_2O_3 to α-Al_2O_3. The difference is that the phase transformation time from θ-Al_2O_3 to α-Al_2O_3 at 1373K is shorter than that at 1273K. In fact, the phase transformation time depends on the oxidation temperature and time /10-15/. With the oxidation temperature increasing, the time needed for transformation from θ-Al_2O_3 to α-Al_2O_3 becomes shorter.

The data for pure NiAl are compiled in the Arrhenius diagram Figure 11 with the data points measured on NiAl-Ag alloy, which shows the Arrhenius lines for the formation of the two mentioned Al_2O_3 modifications. For these alloys k_p decreases rapidly in the temperature range 900-1373K and the k_p for NiAl containing silver is somewhat higher than pure NiAl. The addition of silver gives rise to a rather fine-grained α-Al_2O_3 /16/ layer on NiAl-Ag alloy, and this, on the other hand, causes a relatively higher oxidation rate since the growth of α-Al_2O_3 is mainly by grain boundary diffusion /17/, thus the fine-grained layer grows faster, but not too fast.

Although not obvious from the weight gain kinetics at 1173 and 1273K, surface morphologies are strongly influenced by the minor amount of silver addition. For oxidation at 1173K, the oxides formed on the two alloys containing silver are still whisker-like, but they are shorter and finer than that formed on β-NiAl. After 24h oxidation at 1273K, XRD confirmed the coexistence of θ-Al_2O_3 and α-Al_2O_3, but the dominant oxide is θ-Al_2O_3 on the surface of β-NiAl (Figure 6a). In fact, transformation begins at the metal-oxide interface /18,19/; therefore, the scale may have long whiskers or blades at the scale-gas interface, indicative of cubic aluminas, but still consist of some α-Al_2O_3 beneath this outer layer. In this case, only a very little θ-Al_2O_3 exists on the surface of NiAl-0.5Ag and NiAl-1Ag, whose amount is so small that XRD cannot detect its existence. Comparing the surface morphology at 1273K and that at 1373K, it is obvious that there are two types of α-Al_2O_3, i.e., finer "intrinsic" type and "extrinsic" type, which form as a result of the θ-α Al_2O_3 phase transformation. It is proposed that the "extrinsic" forms when the scale cracks as a result of the volume reduction associated with the phase transformation and at regions where growing α-Al_2O_3 nuclei intersect. These ridges form during the initial transient stage oxidation but do not

grow significantly (relative to scale thickness) during steady-state oxidation. Intrinsic ridges are thought to form on each oxide grain boundary and grow by the outward transport of Al through the scale, during steady-state oxidation /20/.

The corrosion products formed by the oxidation of the present alloys are the same as for the binary NiAl alloy, since silver is noble. Thus the possible effects of the addition of a noble metal A to binary B-C alloys are examined first, assuming that C forms the most stable oxide and that the oxides B and C can dissolve into each other and form double oxides B-C spinel. The oxidation modes of ternary A-B-C alloys of this type should be similar to those of the binary B-C alloys. Relying on the actual alloy composition, these corrosion products include the formation of external BO scales coupled with an internal subscale of CO which contains B-C spinel close to the BO/subscale interface, that of exclusive external layers of CO containing a mixture of BO and B-C spinel, and that of exclusive external layers of CO without the presence of BO and spinel. A new scaling mode is actually possible for ternary A-B-C alloys, i.e. a coupled internal oxidation of B and C, but this is only possible for alloys very rich in A. Apparently, the last scaling mode is not applied to the present ternary alloy because of the relatively low A composition. In all cases of external oxidation, the noble metal A remains in the alloy and becomes enriched at the alloy/scale interface, while at the same time it diffuses back towards the samples interior. Except for the case of simultaneous internal oxidation of B and C, the most important effect of the presence of A can be a reduction of the rate of growth of the external scales as a result of the depletion at the alloy/scale interface of the component forming oxides due to their consumption and to the corresponding enrichment of the component not entering in the scale.

NiAl-0.5Ag and NiAl-1Ag alloys behave as NiAl alloys with a similar overall Ni/Al ratio, except for the possible reduction in corrosion rate due to the decrease of the activities of Al associated with the local enrichment of silver at the scale/alloy interface. The kinetics effect can be excluded in the present cases due to the small solubility of silver in both Ni and Al. In fact, the β phase is essentially composed of a solid solution of nickel and aluminum, so that the effect of silver over its thermodynamic properties can be negligible. Moreover, nickel and aluminum are only slight soluble in silver, so that the phase rich in Ag is composed of practically pure silver. Thus, the two phases of the present NiAl-0.5Ag and NiAl-1Ag alloys have completely different properties, since the α phase rich in Ag is noble and the amount of α phase rich in Ag is very small, while the β phase is essentially equivalent to the binary Ni-Al alloy with the same composition. Neglecting the small solubility of silver in nickel and aluminum and the presence of a small quantity of α phase rich in Ag, the microstructure of the corrosion products of the two alloys are very similar to that of NiAl with the same Ni/Al ratio as observed.

Beneath the oxide scale on NiAl and NiAl-Ag the voids arise for the three alloys oxidized at 1273 and 1373K, except NiAl-1Ag at 1273K, which is attributed to two aspects. On the one hand, the consumption of Al leads to Al depletion beneath the scale, a gradient of the Al concentration and outward diffusion of Al, consequently an opposite gradient of Ni concentration and an inward flux of Ni occur. The loss of Al by oxidation and Ni by inward diffusion may lead to voids. On the other hand, the volatilization of silver at 1373K gives rise to the void formation. These voids will certainly decrease the scale adherence and enhance oxide spalling.

5. CONCLUSIONS

The oxidation kinetics of NiAl-0.5Ag and NiAl-1Ag at 1173 and 1273K is similar to that of β-NiAl. The NiAl-0.5Ag and NiAl-1Ag alloy begin to show weight loss gradually after initial oxidation stage at 1373K due to the volatilization of silver. The oxidation rate is controlled by the growth of different phase Al_2O_3 at different temperatures.

The addition of silver does not affect significantly the scaling behavior of the NiAl intermetallic compound in all cases investigated.

REFERENCES

1. G. W. Goward and D. H. Boone, *Oxid. Met.*, **3**, 475(1971).
2. R. Sivakumar and B. L. McMordie, **37**,139(1989).
3. F. S. Pettit, *Trans. Metall. Soc. AIME*, **239**, 1296(1967).
4. J.L. Smialek, *Metall. Trans.*, **A9**, 309(1978).
5. J. Zhou and J. T. Guo, *Mater. Sci. Eng.*, **A 339**, 166(2003).
6. G. C. Rybicki and J. L. Smialek, *Oxid. Met.*, **31**, 275(1989).
7. J. Doychak, J. L. Smialek and T. E. Mitchell, **20A**, 499(1989).
8. F. S. Pettit, *Trans. Met. Soc. AIME*, **239**,1296(1967).
9. G.C. Wood and F.H. Stott, *Brit. Corros. J.*, **6**, 247(1971).
10. M. W. Brumm and H. J. Grabke, *Corros. Sci.*, **33**, 1677(1992).
11. M. W. Brumm and H. J. Grabke, *Corros. Sci.*, **34**, 547(1993).
12. M. W. Brumm, H. J. Grabke and B. Wagemann, *Corros. Sci.*, **36**, 37(1994).
13. H. J. Grabke and G. H. Meier, *Oxid. Met.*, **44**, 147(1995).
14. H. J. Grabke, D. Wiemer and H. Viefhaus, *Appl. Surface Sci.*, **47**, 243(1997).
15. H. J. Grabke, M. W. Brumm, and B. Wagemann, *Mat. Corros.*, **47**, 675(1996).
16. X. J. Zhang, W. T. Wu, J. T. Guo and Y. Niu, *High Temperature Material and Processes.*, **24**, 17(2005).
17. H. J. Grabke, *Intermetallics*, 7,1153(1999).
18. J. C. Yang, E. Schumann, I. Levin and M. Ruhle, *Acta. Mat.*, **46**, 2195(1998).
19. E. Schumann, *Oxid. Met.*, **43**, 157(1995).
20. B. A. Pint, M. Treska, and L. W. Hobbs, *Oxid. Met.*, **47**, 1(1997).